Tuning of the Charge-Density Wave in the Halogen-Bridged Transition-Metal Linear-Chain Compounds

M. Alouani and J. W. Wilkins
Department of Physics, The Ohio State University, Ohio 43210-1368

R. C. Albers and J. M. Wills
Los Alamos National Laboratory, Los Alamos, New Mexico 87545

(Received 20 April 1993)

Local-density-approximation calculations are used to show that the metal-metal distance along the chains controls the charge-density wave (CDW) in halogen-bridged transition-metal linear-chain compounds. The strength of the CDW can be understood in terms of a two-band Su-Schrieffer-Heeger model if a hard-core ion-ion repulsion potential is also added. We predict a second-order phase transition from an insulating to a semimetallic ground state and explain trends in dimerization, bond-length ratios, band gaps, and Raman breathing modes in terms of the metal-metal distance.

PACS numbers: 71.20.Hk, 71.25.Tn, 71.38.+i, 71.45.Nt

During the past few years halogen-bridged transition-metal linear-chain (MX) compounds have been extensively studied [1–13]. One reason for the increased interest in these materials is that their various competing ground states such as charge-density wave and spin-density wave are sensitive to tuning by chemical substitutions, pressure, or doping [1–11]. In particular, progress has been achieved recently and independently by groups in Japan [4–7] and in Los Alamos [9–11] in tuning the charge-density-wave (CDW) strength over a wide range by using different counterions and equatorial ligands.

In this Letter, we use local-density-approximation (LDA) full-potential linear muffin-tin-orbital (FPLMTO) calculations to study the tuning of the CDW of the MX systems as a function of the metal-metal (M-M) distance along the chain. By comparing experimental results for MX (X =Br, Cl) systems with varying M-M distances to our calculated results for $Pt_2X_6(NH_3)_4$ (X =Br, Cl) under uniaxial stress, we show that *the key parameter* is the M-M distance. Thus, the effect of the different ligands on the properties of these systems is indirect; they tune the M-M distance which is really responsible for the change in the electronic properties. Moreover, we also demonstrate that an extended Su-Schrieffer-Heeger (SSH) model with a universal set of parameters fits the entire class of Pt charge-density-wave MX materials. Thus, we have now provided a crucial theoretical underpinning that explains the CDW MX systems.

Our principal results for the uniaxial stress are as follows: (i) The dimerization, the condensation energy, the Raman breathing mode, and the band gap are gradually reduced, and vanish when the Pt-Pt distance is reduced by nearly 7% from its ground-state value. (ii) Under the same conditions, we predict that the PtBr MX system exhibits a second-order phase transition from an insulator to a semimetal. (iii) The two-band SSH model [14] describes the tuning of the CDW strength *only if* we also introduce a repulsive potential between the metal and halogen ions.

The calculations presented in this paper are based on the LDA with an all-electron scalar-relativistic FPLMTO basis set as described in our previous work [13]. This method was successfully used to show that the dimerization and the insulating ground state of $Pt_2Br_6(NH_3)_4$ are correctly predicted provided that we include the full ligand structure [13]. Under uniaxial stress, we rigidly move the ligands with the metal atoms.

A single MX chain (M= Ni, Pd, or Pt; and X =Cl, Br, or I) consists of alternating MX units, arranged such that two neighboring X atoms move closer to one of the M atoms [1, 2]. This dimerization is schematically represented by $\ldots M^{3-\delta}\ldots XM^{3+\delta}X\ldots M^{3-\delta}\ldots XM^{3+\delta}X\ldots$. Because of the strong electronegativity of the X atoms, the dimerization causes an alternation of the valence character of the metal atoms between $3-\delta$ and $3+\delta$. The strength of the CDW produced is then directly proportional to the dimerization.

Metal-insulator phase transition.—Figure 1 shows the LDA total energy of the PtBr system for Pt-Pt distances less than the experimental lattice parameter (5.55 Å) as a function of the dimerization ξ. Under uniaxial stress, the double-well structure in the energy collapses to a single well, and the condensation energy (the difference between the energy at zero dimerization and the minimum energy) and the dimerization decreases as the Pt-Pt distance is reduced. This agrees with earlier work by Sakai *et al.* on $Pt(en)Cl(ClO_4)_2$ under pressure [4]. At a Pt-Pt distance of 5.18 Å (which is equivalent to a uniaxial stress of 89 kbar based on the first derivative of the total energy versus cell volume) the condensation energy and the dimerization vanish simultaneously, and the system exhibits a second-order phase transition from an insulating to a semimetallic ground state. This is confirmed by the calculated band gap which decreases gradually and closes when the Pt-Pt distance is near 5.18 Å (see the right side of Fig. 2). The possibility of this transition in

0031-9007/93/71(9)/1415(4)$06.00

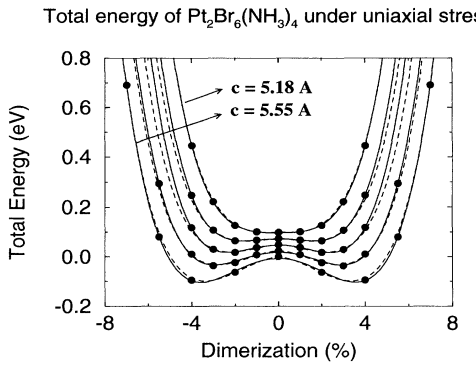

FIG. 1. LDA total energy of PtBr as a function of dimerization ratio ξ (the ratio of half the difference between the two M-X distances to the M-M distance in %) for different Pt-Pt distances. The Pt-Pt distances are, from the upper curve to the lower one, 5.18 Å, 5.29 Å, 5.37 Å, 5.45 Å, and 5.55 Å. The filled circles are the calculated LDA total energies and the full curves are obtained using a polynomial least-squares fit of order 4. The dashed curves represent the total energies as obtained from the Hamiltonian given by Eq. (2) (see text). An energy offset of 0.05 eV instead of the calculated energy offsets has been added between the different curves for clarity of presentation [15]. Under uniaxial stress the size of the dimerization and the dimerization energy are reduced and, at a Pt-Pt distance of 5.18 Å, the dimerization vanishes and a second-order phase transition to a metallic state appears.

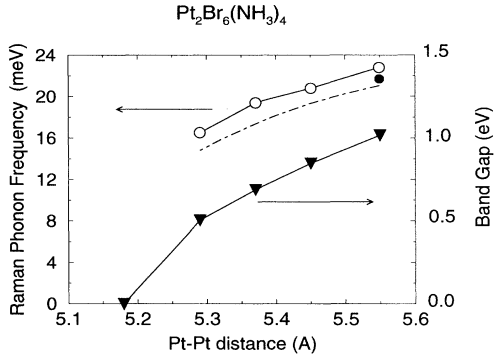

FIG. 2. Calculated (open circles) and measured [1, 11] (filled diamond and circles; the dashed curve is a linear least-squares fit to the experimental data of Ref. [11]) Raman breathing mode, and calculated band gap energy (filled triangles) as a function of the Pt-Pt distance (the experimental band gap under pressure decreases [11] but the absolute magnitude is not yet known). Notice that the linear softening of the breathing phonon mode is in good agreement with the experimental results and with the calculation (long dashed line) using the model of Eq. (2).

$[Pt(NH_3)_4XPt(NH_3)_4X]^{4+}$ chains was first suggested by Whangbo and Foshee using an extended Hückel method [3]. It is also consistent with pressure measurements on the PdBr system, where 140 kbar of hydrostatic pressure caused a nine-order-of-magnitude increase in electrical conductivity [8], due to an increased carrier concentration (because of the reduced gap). However, beyond 140 kbar of pressure a leveling off of the conductivity versus pressure and an increase of the activation energy was observed upon application of pressure up to 350 kbar [8]. Similar conclusions were reached by other researchers [5, 6, 9] for $Pd(chxn)Br(Br)_2$, $Pt(en)Cl(ClO_4)_2$, and $Pt(en)Br(ClO_4)_2$ systems, respectively.

Following the suggestion of Interrante and Bundy [8] that a compression of the metal-ligand bond length may increase the band gap, we have performed self-consistent calculations of the PtCl band structure in which the interchain distance is decreased by 5% without modification of the M-M distance of 5.45 Å along the chain. When the ligand-metal distance is held constant the band gap is unaffected, whereas a 5% decrease in the ligand-metal bond length increases the energy band gap by 0.25 eV. These results coupled with the decrease in the band gap when the metal-metal distance along the chain decreases suggest an *intricate* interplay between the ligand-metal distance and the conduction process along the chain, and may serve as a qualitative explanation for the increase of the band gap beyond some critical pressure. Thus, real pressure is a more complicated situation than the uniaxial pressure generated by chemical subsitutions, where the ligand-metal distance is constant, the CDW state is controlled by the M-M distance, and a metallic state should occur as shown by our calculation.

Softening of the Raman mode.—The use of a harmonic oscillator model in the effective potential given by the total energy curve allows us to estimate the optical (Raman) breathing-mode phonon frequency as a function of the Pt-Pt distance. This breathing mode is an oscillation of the two Br chain atoms around a Pt atom at rest. Since the curvature in the total energy curve (at its minimum) decreases under uniaxial pressure, this frequency is expected to decrease.

Figure 2 displays our calculated Raman phonon frequencies and band gap as a function of the Pt-Pt distance. We observe an almost linear softening of the Raman mode as the M-M distance is shortened. In the vicinity of the phase transition, where the curvature of the total energy becomes flat (cf. Fig. 1) the phonon mode softens considerably. The phonon frequencies for Pt-Pt distances below 5.37 Å are not displayed, because the use of a simple harmonic oscillator to calculate the phonons is dubious since the lattice distortion is comparable to the zero-point motion, and the phonon frequency is comparable to the condensation energy. In this case, thermal effects and zero-point motion, which may cause a breakdown in the Born-Oppenheimer approximation, must be taken into account.

Figure 3 gives a comparison between the calculated short $Pt^{3+\delta}$-X and long $Pt^{3-\delta}$-X bond lengths [X=Br (open circles), Cl (filled circles)] versus the Pt-Pt lattice parameter with the different experimental results

obtained for different MBr/Cl compounds (M=Pt, Pd, and Ni). The different ligands and counterions produce a range of M-M distances for the different compounds. For example, experimentally, substitution of the ClO_4 counterion by Br decreases the metal-to-metal distance along the chain because the hydrogen bond between NH_2 of ethylenediamine (en) or (1R, 2R)-cyclohexanediamine (chxn) ligands and Br counterion is strengthened [7]. The substitution of (chxn) ligand by (en) ligand reduces the metal-metal distance because (chxn) has a nonplanar structure whereas (en) is planar [7].

The experimental results of all these different materials track the calculations under uniaxial pressure. This strongly suggests that the M-M distance is the key parameter controlling the CDW strength.

In addition, the short $M^{3+\delta}$-X bond distance remains essentially constant throughout the series of compounds presented, revealing the contraction of the long $M^{3-\delta}$-X bond as responsible for the large change in the dimerization, therefore reducing the strength of the CDW. Our calculations describe the experimental situation rather well, even though the experimental results are mostly for different MX chain systems with different ligands. But this surprising agreement can be understood qualitatively as follows. In our previous work, we have shown that the dimerization in PtBr system is driven by an electron-phonon coupling confined to a single chain [13]. This strong electron-phonon coupling reduces the short M-X distance to the sum of the ionic radii of the metal and the bridging halogen ions [7]. Thus, the effect of uniaxial stress is to decrease the long M-X bond length which is much softer than the shorter one. To reduce the short bond length, one has to act against the strongly *anharmonic potentials* of the $M^{3+\delta}$ and X ions [16].

We have analyzed quantitatively the effects of uniaxial stress on the strength of the CDW in terms of a two-band single-chain SSH model [12]:

$$H_0 = \sum_{l\sigma}\left\{(-t_0+\alpha\Delta_l)(c^\dagger_{l\sigma}c_{l+1\sigma}+\text{H.c.}) + [(-1)^l e_0 - \beta_l(\Delta_l+\Delta_{l-1})]c^\dagger_{l\sigma}c_{l\sigma}\right\} + \sum_{l,j=0,1} K^{(2j)}_{MX}\Delta_l^{2(1+j)} + \sum_{l,j=0,2} K^{(j)}_{MM}(\Delta_{2l}+\Delta_{2l+1})^{2+j}\,, \quad (1)$$

where $c^\dagger_{l,\sigma}$ ($c_{l,\sigma}$) creates (annihilates) an electron at site x_l with spin σ, and where M and X occupy even and odd sites, respectively. The electron-phonon parameters α, $\beta_{2l}=\beta_M$, and $\beta_{2l+1}=\beta_X$ couple the lattice (through $\Delta_l = x_{l+1}-x_l$) to the electronic structure. The energies $\pm e_0$ and the t_0 are the M and X energy levels and the hopping integral at zero dimerization, respectively. The spring constants $K^{(j)}_{MX}$ between M and X and $K^{(j)}_{MM}$ between M and M model represent elastic energies that model the rest of the electronic structure that is not included explicitly in the one-dimensional electronic structure [17].

The bands in the vicinity of the Fermi energy deviate slightly from the nearest-neighbor tight-binding bands of the SSH model, Eq. (1). Nonetheless, this model, with only *one set* of parameters, fits nicely the relevant bands for any Pt-Pt distance.

Anharmonic potential.—One failure of the SSH model is its prediction of an almost constant ratio of the dimerization to the M-M distance (about 3.6% for PtBr) for all M-M distances, in disagreement with experiment and LDA (which predicts a vanishing dimerization for a sufficiently short M-M distance). We have extended the model by adding a hard-core ion-ion repulsive potential between the metal and halogen atoms along the chain. For simplicity, we have used a next-neighbor repulsive potential. This changes the model Hamiltonian to

$$H = H_0 + \sum_l \frac{2A}{(R^{(0)}_{MX}+\Delta_l - R_c)^q}\,, \quad (2)$$

where A and q are constants representing the strength

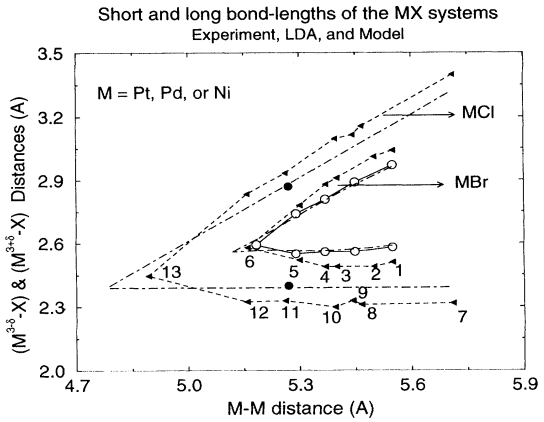

FIG. 3. LDA calculated short $M^{3+\delta}$-X and long $M^{3-\delta}$-X bond lengths for $Pt_2Br_6(NH_3)_4$ (open circles) and $Pt_2Cl_6(NH_3)_4$ (filled circles) as a function of M-M distance. The filled triangle symbols represent experimental data for various MX systems [7,10]: 1-$Pt_2Br_6(NH_3)_4$; 2-[Pt_2(en)$_4Br_2$] $(ClO_4)_4$; 3-[Pd_2(en)$_4Br_2$] $(ClO_4)_4$; 4-[Pt_2(chxn)$_4Br_2$] $(Br)_4$; 5-[Pd_2(chxn)$_4Br_2$] $(Br)_4$; 6-[Ni_2(chxn)$_4Br_2$] $(Br)_4$; 7-[Pt_2(chxn)$_4Cl_2$] $(ClO_4)_4$; 8-[$Pt_2Cl_2(NH_3)_8$] $(HSO_4)_4$; 9-[Pt_2(en)$_4Cl_2$] $(ClO_4)_4$; 10-[Pt_2(tn)$_4Cl_2$] $(BF_4)_4$; 11-[Pt_2(en)$_4Cl_2$] $(CuO_4)_4$; 12-[Pt_2(chxn)$_4Cl_2$] $(Cl)_4$; 13-[Ni_2(chxn)$_4Cl_2$] $(Cl)_4$. The solid and dashed curves are guides to the eye. The dot-dashed curve is the result predicted by the model of Eq. (2). Notice that the calculated and measured short M-X bond lengths are roughly independent of the M-M distance and that the agreement between the calculations and the experimental results is good.

TABLE I. Parameters of the model given by Eq. (2) obtained from the fit to the LDA results. The units of $2e_0$ and t_0 are eV, those of α are eV/Å, and those of $K^{(j)}$ are eV/Å^{j+2}. The β parameters are found to be zero.

	$2e_0$	t_0	α	$K^{(0)}_{MX}$	$K^{(2)}_{MX}$	$K^{(0)}_{MM}$	$K^{(1)}_{MM}$	$K^{(2)}_{MM}$	A (meV)	R_c (Å)	q
PtBr	2.3	1.5	2.4	0.007	7.0	2.2	-2.6	-2.0	7.0	2.0	3
PtCl	2.9	1.6	2.3	0.0	1.7	3.9	-5.5	-16.0	9.4	1.8	3

and hardness of the potential, $R^{(0)}_{MX}$ is the M-X distance at the experimental equilibrium ground state at zero dimerization, and R_c is a hard-core distance between M and X [18].

The Hamiltonian of Eq. (2) fits the LDA total energy of PtBr under uniaxial stress rather well (see Fig. 1, dashed curves). The parameters used to describe the LDA total energies are [19] given in Table I. In Fig. 3 we have also depicted the short $M^{3+\delta}$-X and the long $M^{3-\delta}$-X bond lengths predicted by the model given by Eq. (2) as a function of the Pt-Pt distance. Notice that the model is in good agreement both with the LDA and the experimental results. So, the constant $M^{3+\delta}$-X short bond is explained as a result of the *competition* between a strong *electron-phonon coupling* acting along the chain and a *hard-core repulsive potential* between the metal and halogen ions.

To further illustrate the model given by Eq. (2), we have calculated the short and long bond for PtCl. The LDA is used to get the dimerization for the ground state (Pt-Pt distance of 5.27 Å [20]), then the model is fitted to the LDA results with the requirement that the short bond length is equal to the LDA prediction. This procedure provided the model parameters shown in Table I. Figure 3 shows that our prediction for PtCl compares favorably with the available experimental results. The model also predicts a metallization for PtCl at a Pt-Pt distance of 4.78 Å. Notice that the Ni-X sytems (numbers 6 and 13 in the figure) do not dimerize; in fact, they are magnetic, which opens a gap that prevents them from being metallic.

In conclusion, we have found that LDA correctly predicts the variation in CDW strength of PtBr and PtCl under uniaxial stress, and that the key parameter is the M-M distance. We have shown that the dimerization, the band gap, and the breathing phonon mode all decrease linearly with the M-M distance in agreement with experiments for related systems [4–11]. At a Pt-Pt distance close to the sum of the ionic radii a second-order phase transition to a metallic state appears.

Finally, we have shown that the SSH model required the addition of a hard-core repulsive potential between the metal and the halogen ions to reproduce the correct tuning of the CDW strength in the MX systems. This shows that the constant short $M^{3+\delta}$-X distance is an equilibrium distance resulting from a *competing* strong electron-phonon coupling and a hard-core repulsive potential between the metal and the halogen ions.

We thank R. H. Mckenzie for stimulating discussion. Partial support was provided by the Department of Energy (DOE)–Basic Energy Sciences, Division of Materials Sciences. Supercomputer time was provided by the Ohio Supercomputer and by the DOE.

[1] H. J. Keller, in *Extended Linear Chain Compounds*, edited by J. S. Miller (Plenum, New York, 1983), Vol. 1, p. 357.
[2] R. J. H. Clark and R. E. Hester, in *Infrared and Raman Spectroscopy*, edited by R. J. H. Clark and R. E. Hester (Heyden, London, 1984), Vol. 11, p. 95.
[3] M. H. Whangbo and M. J. Foshee, Inorg. Chem. **20**, 113 (1981).
[4] M. Sakai *et al.*, Phys. Rev. B **40**, 3066 (1989).
[5] N. Kuroda *et al.*, Phys. Rev. Lett. **68**, 3056 (1992).
[6] H. Okamoto *et al.*, Synth. Met. **41–43**, 2791 (1991).
[7] H. Okamoto *et al.*, Mater. Sci. Eng. B **13**, L9 (1992), and references therein.
[8] L. V. Interrante and F. P. Bundy, J. Inorg. Nucl. Chem. **39**, 1333 (1977), and reference therein.
[9] R. J. Donohoe *et al.*, in *Frontiers of High Pressure Research*, edited by H. D. Hochheimer (Plenum, New York, 1991).
[10] B. Scott *et al.*, Synth. Met. (to be published).
[11] G. S. Kanner and B. I. Swanson, Bull. Am. Phys. Soc. **38**, 258 (1993).
[12] J. T. Gammel *et al.*, Phys. Rev. B **45**, 6408 (1992), and references therein.
[13] M. Alouani et al., Phys. Rev. Lett. **69**, 3104 (1992).
[14] W. P. Su *et al.*, Phys. Rev. B **22**, 2099 (1980).
[15] The energy offsets between the curves at zero dimerization, from top to bottom, are 0.32 eV, 0.17 eV, 0.13 eV, and 0.22 eV/(unit cell). The total energy versus the Pt-Pt distance produced a global minimum at 5.71 Å and a dimerization of 4.2%. The experimental Pt-Pt distance and dimerization is 5.55 Å and (4.8–5.2)%, respectively [1, 2]. In Fig. 1 only total energies corresponding to Pt-Pt distances below the experimental lattice parameter are shown.
[16] The PdX and PtX compounds have the same M-X short distance because their ionic radii are almost identical [see R. D. Shannon and C. T. Prewitt, Acta Crystallogr. Sect. B **25**, 925 (1969)].
[17] The $K^{(2j+1)}_{MX}$ are zero because the total energy is even with respect to the dimerization.
[18] The fit is insensitive to the parameter q, and the parameter R_c is directly proportional to the sum of the radii of the metal and the halogen ions.
[19] The parameters e_0, t_0, α, β_M, and β_X are kept fixed to the values obtained from the fit to the LDA band structure under uniaxial stress.
[20] G. M. Summa and B. A. Scott, Inorg. Chem. **19**, 1079 (1980).